Pisco Med Publishing

The Method of False Vortices in Designation Problems of Targets, road Signs, Facial Features and Real Vortices in Space Images

E. N. Terentiev[1], I. García-Magariño [2], N. E. Shilin-Terentyev[3], I. N. Prikhodko[1] and I. I. Farshakova[1]

[1] Department of Computer Modeling and Informatics, Faculty of Physics, M.V.Lomonosov Moscow State University, Moscow, Russia

[2] University of Zaragoza, Zaragoza, Aragon, Spain

[3] Google, San Francisco, CA, USA

Abstract: An image in one color is a scalar field. The image is associated with its vector gradient field. The analysis of vector fields with the help of single-length vector templates made it possible to indicate in the image such objects as vortices, Road Signs (RS), Facial Features (FF), and so on. The proposed method of indicating local objects using gradient fields turned out to be highly accurate and noise-proof. The presented advantages of the proposed method recommend it as a promising tool in targets designation problems.

Keywords: Mage Analysis; Localization of Object in the Image; Computer Vision; Designation Problems of Targets; Road Signs; Facial Features; False Vortices;

1. Introduction

The task of localizing objects in an image is one of the basic tasks of computer vision. The task can be considered as consisting of two tasks: finding the candidate's location in the desired object class and its subsequent classification. Problems of this type include: problems of recognition of RS, described in many articles[1-9] problems search for vortices[10], detection of person's face in article[11], etc.

Popular approaches to the localization of objects, for example, RS, based on methods of contour analysis[1], or combined with color segmentation of the image, as in[2], have problems in the accuracy and stability of localization. As a result of poor illumination of the objects, the areas of the candidate for RS in the image are inaccurate, with the loss of a part of the RS, or vice versa, the area of the RS candidate is chosen too large. What makes it impossible to further classify the object. Estimation of the location of the object is given by morphlets, which are a special modification of the methods of morphological analysis[12]. Used in various articless[3-8] methods of classification of RS, like neural networks[3,4,6], contour descriptors[5], color histograms[9], the search for key points[7] have their problems in the accuracy and stability of classification in their specific tools, terms. The use of precise localization methods with the estimation of the sizes of objects that are stable to the conditions of registration will make it possible to improve the accuracy of classification, reading, for example, RS.

2. Finite-dimensional Sampling Theorems with operations of differentiation and integration

Finite-dimensional Sampling Theorems (FDST) realize interpolation operations, field theories with sample arrays with a mantissa accuracy of the order of ~ 10^{-13} without using finite difference schemes and integral

doi: 10.18282/ics.v1i1.594

sums.

2.1 2D FDST (Terentiev):

Let there be given: a square array of samples (the image on the original grid NxN) D = f (x0, y0), the two-dimensional orthonormal matrix of the discrete Fourier harmonics H (0) (x0) = {Hk (0) (x0), k = 1: N , x0 = 0: N-1} and the interpolated Fourier harmonics H (n) (x) = {Hk (n) (x), k = 1: N, x = 0: dx: N-dx}, with a smaller step dx <1.

All Fourier harmonics are numbered first - k index and in the discrete matrices H (0) (x0), dx = 1 and in the interpolated matrices H (n) (x), dx <1. The Fourier harmonics are arranged in rows.

The subscripts in parentheses (n) are the n-th (for positive n> 0) derivatives and the –n-th integral for negative values[13].

Then the function:

$$f^{(n,m)}(x,y) = \sum_{i,j=1}^{N} c_{i,j}\, H_i^{(n)}(x)\, H_j^{(m)}(y) \qquad (1)$$

$$c_{i,j} = (f(x0,y0), H_i^{(0)}(x0)\, H_j^{(0)}(y0)) = \\ = \sum_{x0,y0=1}^{N} f(x0,y0)\, H_i^{(0)}(x0)\, H_j^{(0)}(y0),\ i,j = 1:N \qquad (2)$$

passes through the sample points f (x0, y0) for n = m = 0.

The scalar products (2) realize the two-dimensional Direct Fourier Transform (DFT). The Fourier series f (n, m) (x, y) (1) gives us an interpolated two-dimensional result for n = m = 0, dx <1. If there is no interpolation: dx = 1 and n = m = 0, then the Fourier series f (n, m) (x, y) (1) realizes the Inverse FT. If n and m are not equal to zero, then we implement the operations of differentiation and integration from the sample arrays[13]. Note that the orders of the operations n, m are not necessarily integers[13].

1D FDST: ***Suppose*** we have a one-dimensional array of samples D = f (x0), ***then*** the result of interpolation with the n-th operation is represented by the formula in one line:

$$f^{(n)}(x) = (H^{(0)}(x0) * D')' * H^{(n)}(x) \qquad (3)$$

An asterisk * in (3) denotes the rule "string * column with summation" when multiplying matrices and a prime 'is the transpose operation.

The first asterisk realizes a one-dimensional DFT (2), and the second asterisk is the sum of a discrete Fourier series (1). Note that the matrices of digitized Fourier harmonics H (0) (x0) are unitary in construction and are intended for the realization of one-dimensional FTs. If n = 0 and x = x0, then the original equation f (x0) = f(0) (x0) = D follows from the fact that the matrix H(0) (x0) is unitary (the transpose operation reverses the unitary matrix).The FDSTs give good results if there is no difference in image boundary. Otherwise, it is necessary to apply special methods protected from boundary effects in the FDST[13].

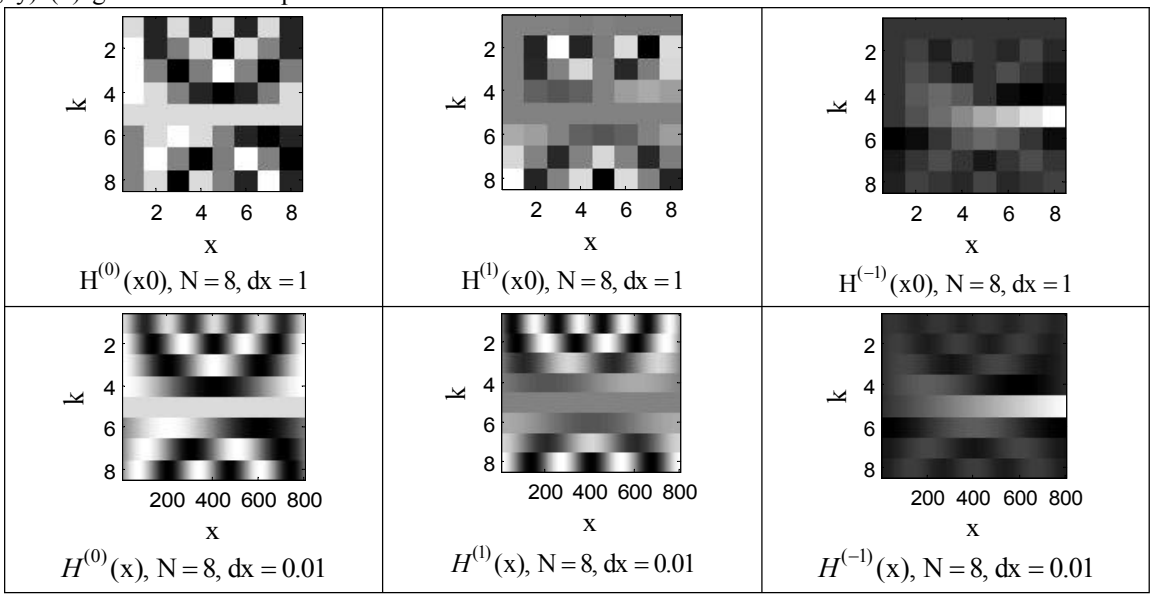

Figure 1; Example of discrete and interpolated, differentiated and integrated Fourier harmonics in the FDST**.**

Below, we give formulas with operations of differentiation and integration of the n-th order for sines and cosines:

$$H_k^{\cos^{(n)}(\rho_m x)} = \sqrt{2/N}\,\{(\rho_m)^n \cos(\rho_m x + n\frac{\pi}{2})\},$$
$$\rho_m = \frac{2\pi}{N}m,\ \ m = \frac{N}{2} + 1 - k, \tag{4}$$

$$H_k^{\sin^{(n)}(\rho_m x)} = \sqrt{2/N}\,\{(\rho_m)^n \sin(\rho_m x + n\frac{\pi}{2})\},$$
$$\rho_m = \frac{2\pi}{N}m,\ \ m = k - (\frac{N}{2} + 1), \tag{5}$$

In (4.5), the index k = 1: N indicates the line numbers in the matrix of continuous Fourier harmonics $H^{(n)}(x)$, see **Figure 1** for even N with $\sqrt{2/N}$ normalization. For the lines of the unpaired cosine and the constant in $H^{(0)}(x0)$, another normalization is $\sqrt{1/N}$.

The normalizations from the discrete case are necessary for the orthonormality of the rows of the matrix $H^{(0)}(x0)$[13].

3. Gradient fields, direction templates, vector operations

According to the 2D FDST (1.2), the gradient from the sample array D = f (x0, y0) with interpolation at the points (x, y) is:

$$gD = gradD = \{\frac{\partial}{\partial x}D, \frac{\partial}{\partial y}D\} = \{f^{(1,0)}(x,y), f^{(0,1)}(x,y)\} \tag{6}$$

gD (6) – there is a vector gradient field associated with the scalar image D.

In **Figure 2** graphically represents the steps of the proposed method of "vector analysis of images." For image analysis, it is often convenient to consider orthogonal or rotated in $\pi/2$ to a vector field ogD.

The analysis of the shape of vector fields is performed using two given templates of vector fields with unit directions along the radius and circumference [diR], [diC].

The second and third cells of Figure 2 shows how the projection operations P = P_X are implemented, on the direction template X = [diC].

The projection Pf is called a signal, and the orthogonal part of f-Pf - by noise. There is a revers operation for vectors f, i.e. change the direction of the vector f by the opposite -f operation if (f, diC) <0, then if between the vectors f and dC is an obtuse angle.

Similarly, vectors can rotate in templates: from the template of directions along the radius [diR], we can obtain a template of directions along the circle [diC], see **Figure 2.**

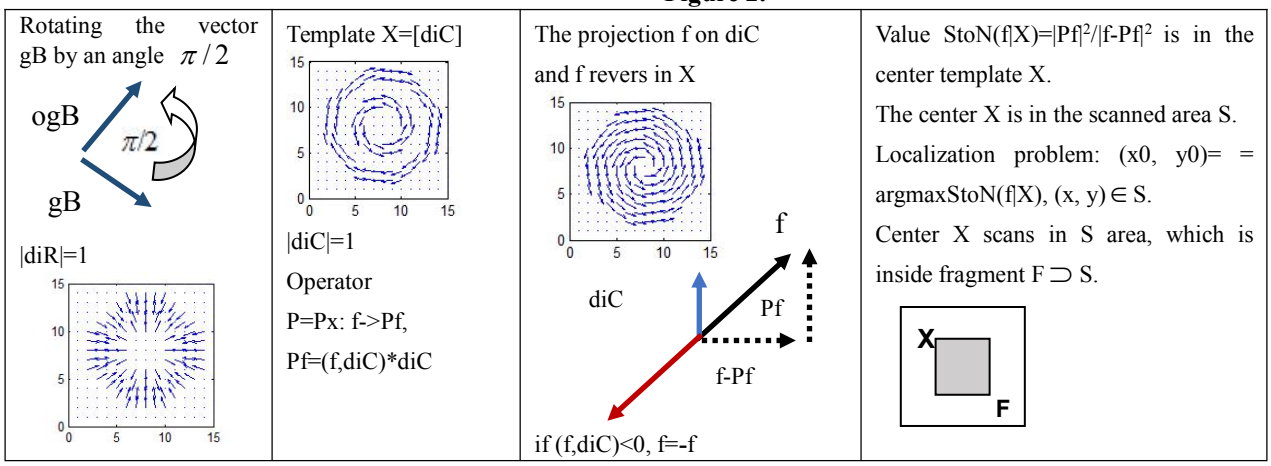

Figure 2; Operations on vector fields, templates, projections, StoN function - "Signal / Noise"**.**

Imagine, in image B, a bright ring is a scalar array B. Then ogB will represent two vector fields rotating in opposite directions. Of course, either we design a similar template to define the ring, or we allow the revers operation and remain with the simple direction template X = [diC], as in **Figure 2**. The advantage of this approach is that we can have a larger-sized template than the required ring and steadily realize the localization, without loss of the object.

4. Object localization problem

Let's write the signal-to-noise ratio StoN:

$$StoN(f|X)=||Pf||^2/||f-Pf||^2 \quad (7)$$

Note that StoN (7) can have an infinite value if the part with noise $||f-Pf||^2 = 0$, for example, for f = X. Therefore, we will use the MatLab function atan2 (arcctg):

$$aStoN(f|X)=\pi/2 *atan2(||Pf||, ||f-Pf||) \quad (8)$$

The function aStoN with normalization on $\pi/2$ (8) will be used later in estimating the parameters of real vortices.

The center of the template X scans in the region S in the image fragment F of the image. The values of functions of the StoN, aStoN type (7.8) are associated with the coordinate (x, y) in the S part F of the image fragment. The point (x0,y0) of the maximum of the function StoN (x,y), $(x,y) \in S \subset F$ determines the positions of the object of interest in the image. The quality or accuracy of localization can be estimated by the size of the light part or the "radius of spot" in the image of the StoN function.

Thus, the problem of localizing or determining the coordinates (x0, y0) of an object reduces to the roblem on maximum:

$$(x0,y0)=argStoN(f|X)(x,y), (x,y) \in S \quad (9)$$

5. General scheme of application of the method

Let's consider the principle of the method in stages. In fact, this scheme is presented in **Figure 2**, but with the addition of the task of filtering images in the second stage. When filtering, the High Frequency (HF) part of the image is cleared and the Low Frequency (LF) part is left for use. This is necessary for a more stable work of the method, together with the use of simplified templates with the operation revers.

Stages of general schem:

1. The device measures or reads the input image B;
2. It sets to zero HF part of the image;
3. The device's processor calculates the vector gradient field gB = grad B.
4. It rotates all vectors of the vector field gB by an angle $\pi/2$ to obtain an orthogonal vector field f = ogB ..
5. It projects a vector field f = ogB in the direction of X, P = PX, to obtain the signal vector part Pf and the noise vector part - f-Pf;
6. It calculates the signal-to-noise ratio StoN (7,8) at each point of the scanning region of the template X in S. The object sought is presumably in S;
7. It finds the coordinates (x0, y0) of the desired object corresponding to the pattern X, solving the problem to the maximum (9)

So, the scheme or algoritm of realization of a sequence of vector operations over the gradient field of the image is given, which gives the coordinates of the location of the object of the sought class in the images. Of course, all this is the content of the general problem of target designation.

6. Example of indication of vortices

Next, examples of the localization of objects of different classes will be demonstrated: vortices, RS, chamomile flowers and Pupil of the Eye (PE). If it is possible to say about RS, PE that the forms of RS, PE are standard, they are known. Vortices can not be attributed to objects whose form is known.

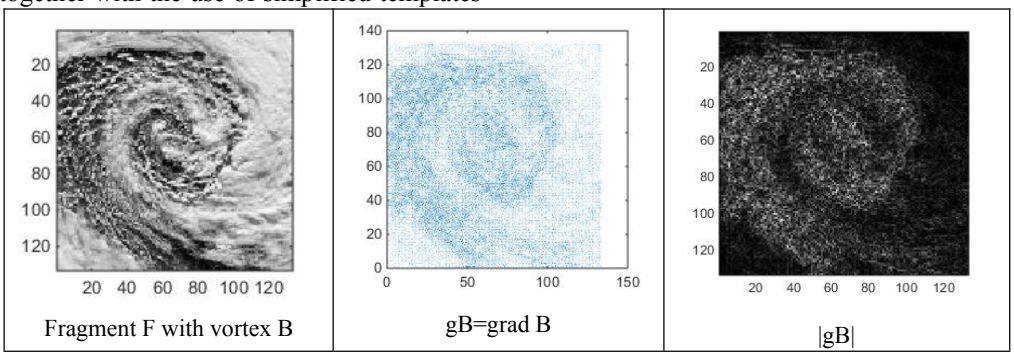

Figure 3; An example of a fragment F with a vortex B, a gradient field gB and | gB |.

Let us take a fragment of a space image containing an atmospheric vortex, see **Figure 3**. The vortex is identified by a vector template X = [diC], indicating the location by the maximum of the function StoN (7) in the scanning region S shown in **Figure 3-6**.

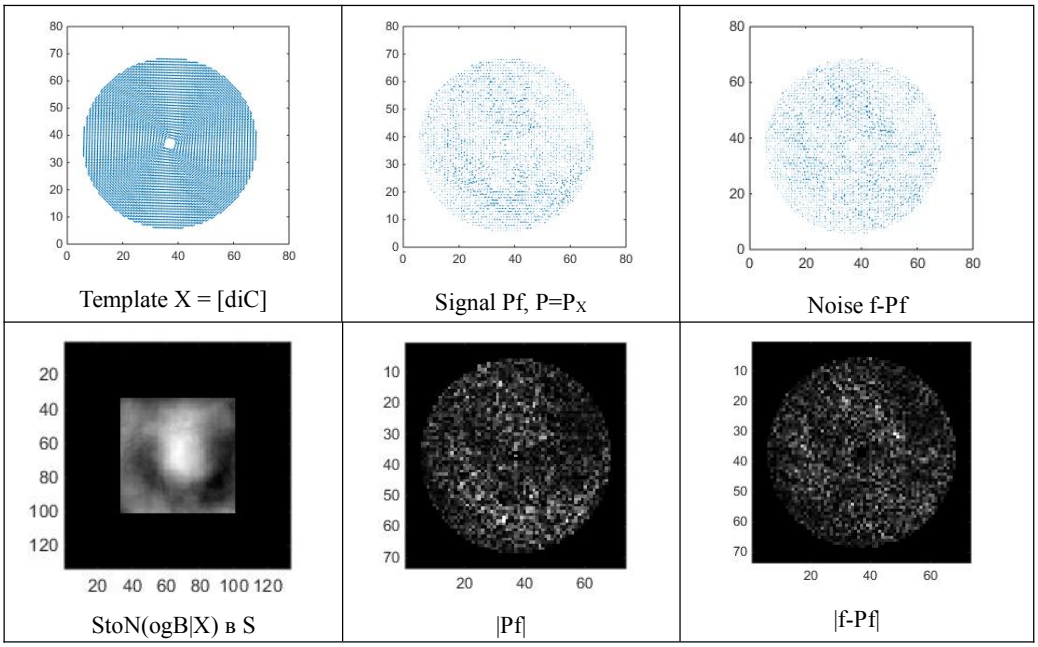

Figure 4; Components of the StoN function for the vortex and its value in the scanning region S**.**

If you set to zero ~70% of the HF image, ~30% of the LF is the reminder image, the vortex localization method remains operational, see **Figure 5-6**.

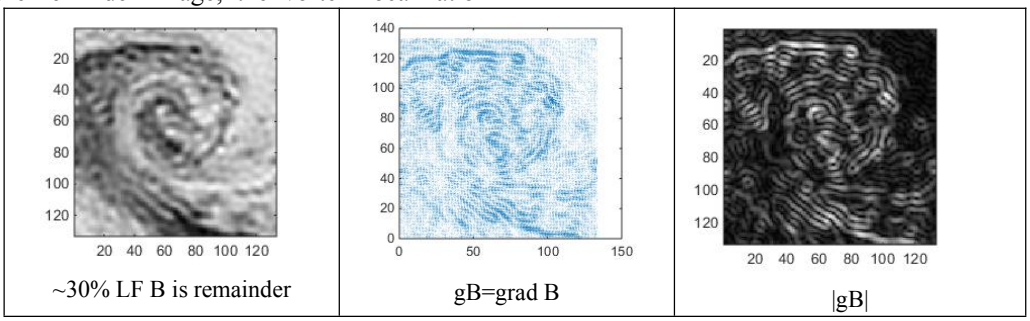

Figure 5; An example of a 30% LF image with a vortex B, a gradient field gB, and | gB |**.**

In the construction of the functions StoN (7), in essence, the ratio of the energy of the circular motion is taken - the signal part to the radial motion energy - the noise part.

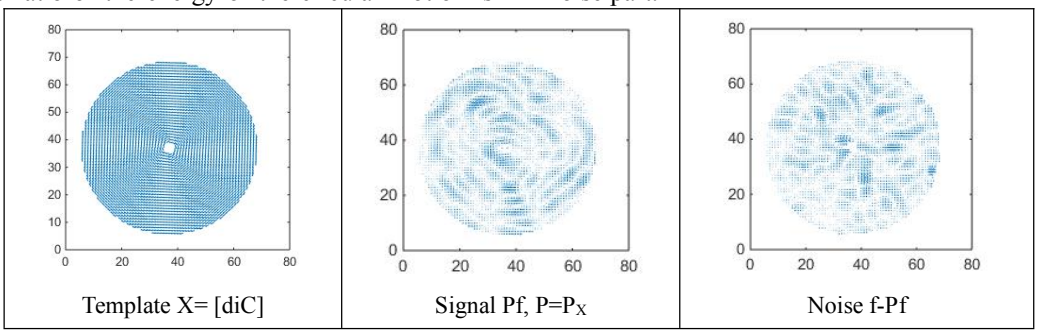

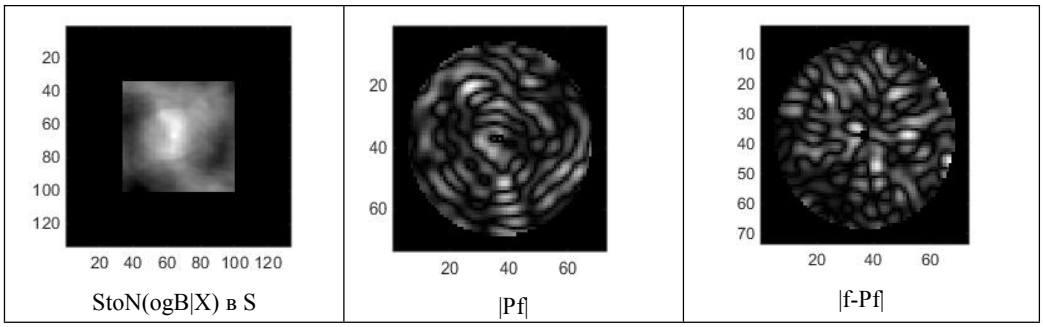

Figure 6; Components of the StoN function for a vortex with 30% LF image and its values in the scanning area S**.**

7. False vortices and their applications

If as an input image to take images of a chamomile flower, then the method will have the same reaction to the chamomile as to the vortex. Therefore, it can be said that the image of a daisy flower is a false vortex for a real vortex.

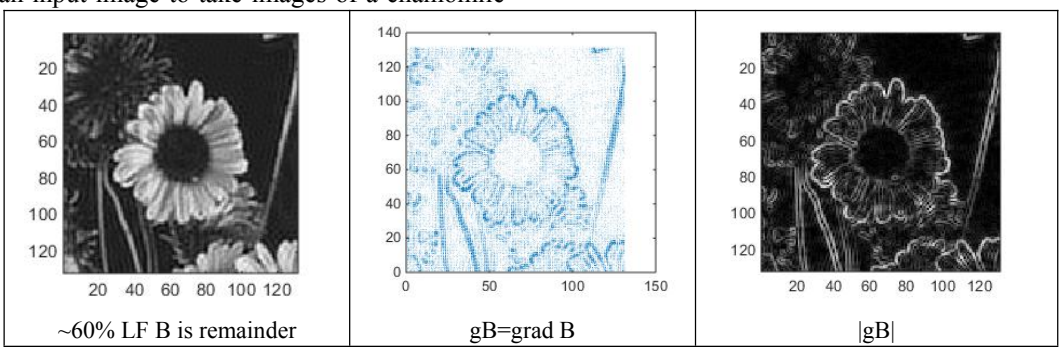

Figure 7; An example of an image area with chamomile B, a gradient field gB and | gB |**.**

In space images, gradients or pressure drops, in the direction of which the air masses move, are not fixed. Therefore, the vortex localization method not only fixes vortices. By the way, to allocate flowers of a camomile and a cornflower in a bouquet of flowers, as false whirlwinds with an eye and without an eye, it appears possible.

On scalar space images, it is required to monitor the state of the atmosphere with the indication of vortices in the atmosphere. The proposed method allows you to do this automatically.

And in the case of chamomile flower, the zeroing of the HF image improves the result. In 60% of the LF part, the result is even better than in the entire frequency band.

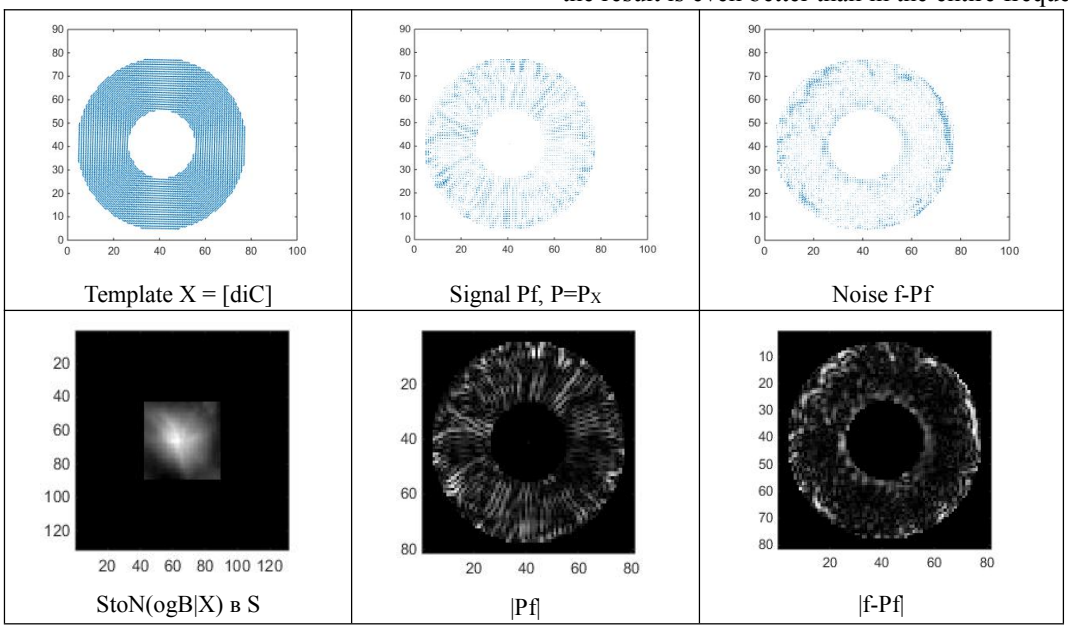

Figure 8; Components of StoN function for chamomile flower and its values in the scanning area S**.**

A false whirlwind "around the perimeter of a triangle" allows you to localize the RS even if 30% of the LF remains from the image. In Blue (B), as an additional to the Red R, the picture | gB | looks more contrast than | gR |.

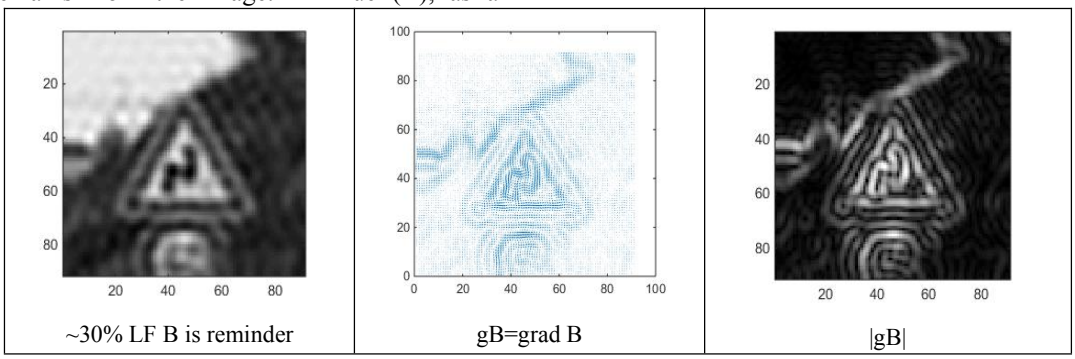

Figure 9; An example of the image region B (Blue) with RS, the gradient field gB and | gB |**.**

Another round RS, which is located lower prevents the localization of triangular RS, see **Figure 9** and **Figure 10**.

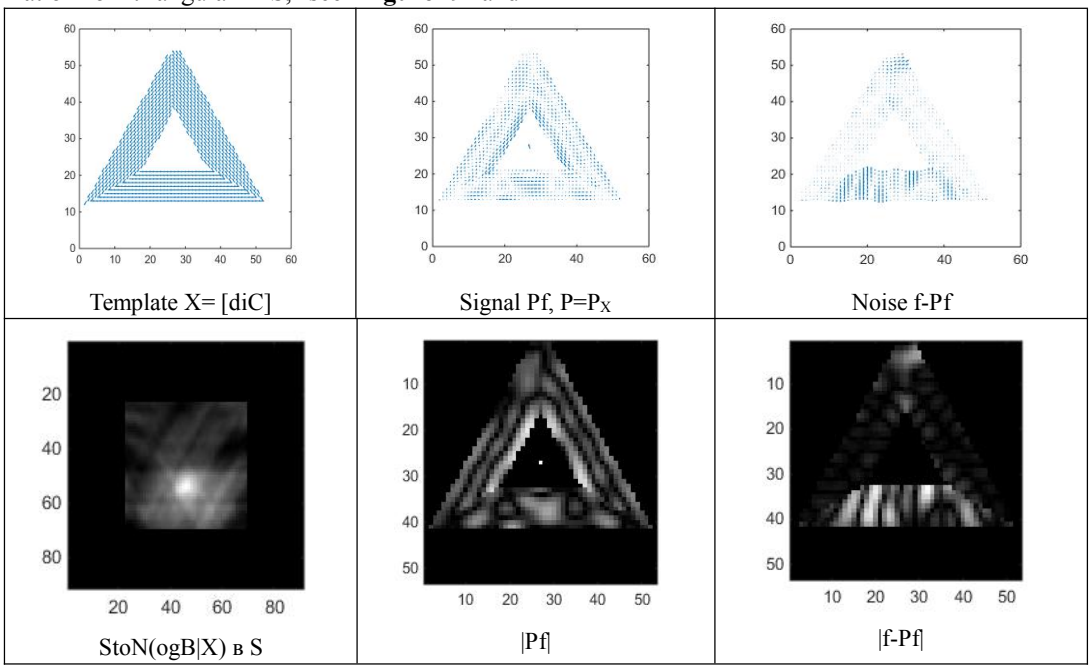

Figure 10; Components of the StoN function for RS and its values in the scanning area S**.**

In the problem of recognizing faces or in the problem of the Facial Features (FF), the distance between the Pupils of the Eyes (PE) in the image is the unit for measuring distances. All other elements of the FF can be found with the distance from the PE and with the help of this vector method for the analysis of other FF.

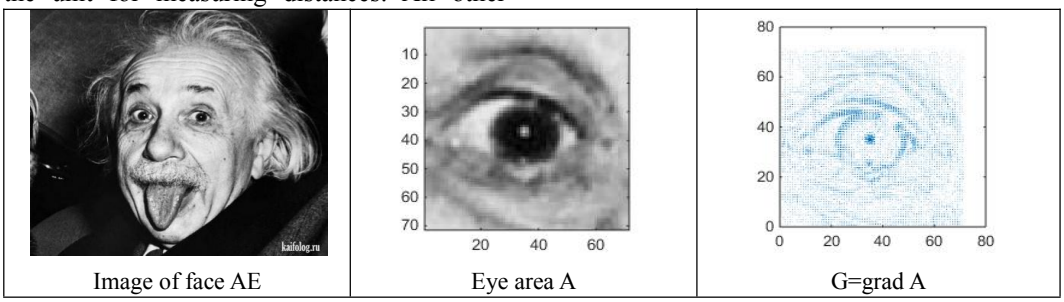

Figure 11; Initial face image AE, eye area A, gradient field G**.**

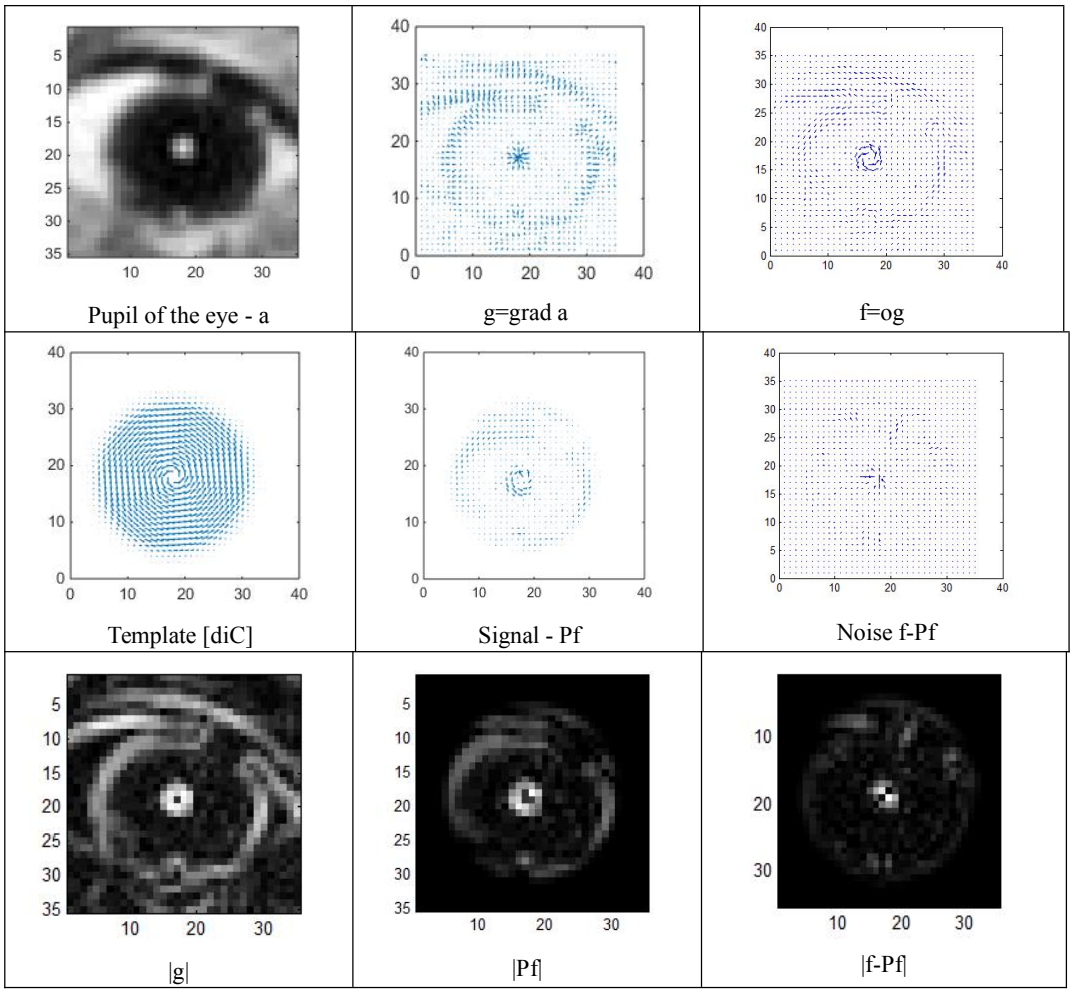

Figure 12; Components of vector operations in the area of the PE**.**

The quality of the localization of objects in the region S (7) can be estimated by the size of the bright spot in the image of the StoN function. We calculated StoN functions in three ways.

The first was to localize the PE by the method of morphological analysis of the images (by areas) and to the input image of the fragment of eye A, see **Figure 11** and **Figure 13**. The second method is the modernized morphological analysis of images, in which the "PE contours" were distinguished by a gradient method (see **Figure 12**, | g |) and then StoN was constructed in the area of the contours in | G |.

The smallest spot was obtained in the third compared method StoN (oG | X) (see **Figure 13**), which is represented in this paper. We believe that this method is applicable to the solution of the complex problem of face recognition from images or specifically from the FF. There are ideas to realize the semantic analysis of images of the FF: nose, lips, PE region, ears, etc. using gradient fields and vector transformations.

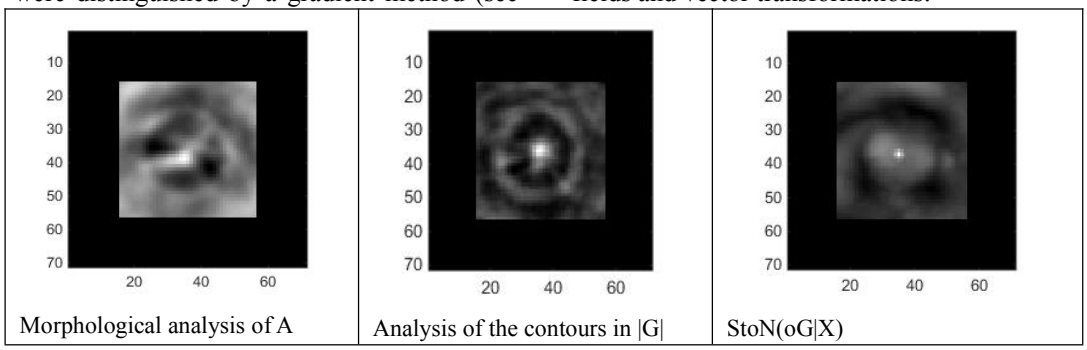

Figure 13; Comparison of StoN functions in the scanning area S by different methods**.**

8. Discussion

With the proposed approach, we were able to determine the location of objects with irregular and regular properties such as vortices and RS, which suggests that the proposed method is universal for the search for a wide class of objects. An unexpected result of the investigation is that gradient methods with projections on given templates of directions made it possible to indicate quite accurately with the aid of false vortices various objects of the type of RS. In real problems of reading RS in the preliminary task, together with the evaluation of the place of the RS, it is of course necessary to evaluate the size of the candidate in the RS. The ability to accurately assess the localisation of the RS opens new avenues for solving the problem of semantic analysis of images such as reading the RS by the Robot Navigator.

Estimating the exact distance between the PE makes it possible to formulate new semantic problems in estimating the parameters of the FF type for the realization of methods for recognizing face images of individuals. In the plans of the problem of estimating the parameters of atmospheric vortices and dipole eddies of sea currents[15] in space images of the Earth.

In the plans to implement the diagnostic task for the presence of tumors, ulcers, etc. in medical images, including in tomography by the method of false vortices.

Using the well-known sampling theorem of Wiener-Kotel'nikov[16], it is impossible to repeat the results of the FDST[13].

In our studies, it turned out that the realized accuracy was excessive and, to improve the result, we reset the HF images - coarsened images.

It is necessary to investigate, for example, double anti-vortices in templates X, see Figure 2, to determine the position of the RS with a maximum accuracy of one pixel and less.

The limiting accuracy of localization can be achieved if done with interpolation and less to zero the HF images. We believe that this can happen on RS images and in the designation problems.

References

1. Hai Nguyen Thanh // Electrical and Electronic Engineering, 2014. 4(2): 36-44
2. Шемарулин И.А., Карпычев В.Ю. // Труды НГТУ им. Р.Е. Алексеева. 2016. № 2. Р. 60, (in Russian).
3. Shustanov A., Yakimov P. // Proceedings of the 14th International Joint Conference on e-Business and Telecommunications. 2017. 5, P. 42.
4. Krsak E., Toth S. // Acta Electrotechnica et Informatica. 2011. 11, №,4. P. 31.
5. 5 Keser T., Kramar G., Nozica D. //In Proceedings of the IEEE International Conference on Smart Systems and Technologies (SST), 2016. Osijek, Croatia, 12-14.
6. Xiong B., Izmirli O. // International Workshop on Image Processing and Optical Engineering, International Society for Optics and Photonics. 2012. 8335, P. 83350B.
7. Hla Myo Tun Htet Wai Kyu, Lu Maw // INTERNATIONAL JOURNAL OF SCIENTIFIC and TECHNOLOGY RESEARCH, 2016. 5, ISSUE 06.
8. Приходько И.Н. // XXV Международная конференция студентов, аспирантов и молодых учёных по фундаментальным наукам "Ломоносов - 2018". Секция "Физика", 2018, (in Russian).
9. Daraghmi Y-A, Hasasneh A. M. // International Journal of Signal Processing Systems. 2016. 4, № 5, pp. 417-421
10. Алексанин А.И., Загуменнов А.А. // Современные проблемы дистанционного зондирования Земли из космоса. 2008. В.5. Т.2. С. 17-21, (in Russian).
11. Liao S., Anil K. J., Stan Z.Li. // IEEE Trans. Pattern Analysis and Machine Intelligence. 2015.
12. Визильтер Ю.В., Горбацевич В.С., Вишняков Б.В., Сидякин С.В. // Компьютерная оптика, 2017, 41, № 3, (in Russian)
13. Е.Н. Терентьев, Н.Е. Терентьев // ПРОЦЕССЫ В ГЕОСРЕДАХ. 2016. №4(9), с.355-362, (in Russian).
14. Пытьев Ю.П., Чуличков А.И. Методы морфологического анализа изображений. М.:Физматлит, 2010, (in Russian).
15. Терентьев, Н.Е. Терентьев, И.И. Фаршакова // Труды школы-семинара «Волны-2017». Математическое моделирование в радиофизике и оптике. 2017. с.56-58, (in Russian).
16. Кузнецов Н.А., Синицын И.Н. "Развитие теоремы отсчётов Котельникова" УФН179 216–218 (2009), (in Russian).